AUTHOR(S):

Nishizuka, K; Funato, M; Kawakami, Y; Fujita, S; Narukawa, Y; Mukai, T

# Efficient radiative recombination from $\langle 11\bar{2}2 \rangle$ -oriented In$_x$Ga$_{1−x}$N multiple quantum wells fabricated by the regrowth technique

K. Nishizuka,[a] M. Funato, Y. Kawakami, and Sg. Fujita
*Department of Electronic Science and Engineering, Kyoto University, Kyoto 615-8510, Japan*

Y. Narukawa and T. Mukai
*Nitride Semiconductor Research Laboratory, Nichia Corporation, Tokushima 774-8601, Japan*

In$_x$Ga$_{1−x}$N multiple quantum wells (QWs) with [0001], $\langle 11\bar{2}2 \rangle$, and $\langle 11\bar{2}0 \rangle$ orientations have been fabricated by means of the regrowth technique on patterned GaN template with striped geometry, normal planes of which are (0001) and $\{11\bar{2}0\}$, on sapphire substrates. It was found that photoluminescence intensity of the $\{11\bar{2}2\}$ QW is the strongest among the three QWs, and the internal quantum efficiency of the $\{11\bar{2}2\}$ QW was estimated to be as large as about 40% at room temperature. The radiative recombination lifetime of the $\{11\bar{2}2\}$ QW was about 0.38 ns at low temperature, which was 3.8 times shorter than that of conventional [0001]-oriented In$_x$Ga$_{1−x}$N QWs emitting at a similar wavelength of about 400 nm. These findings strongly suggest the achievement of stronger oscillator strength owing to the suppression of piezoelectric fields. © *2004 American Institute of Physics.* [DOI: 10.1063/1.1806266]

Nitride-based light-emitting diodes (LEDs) have already been commercialized for the violet to green spectral range.[1,2] It is often reported that there are two competitive factors determining the internal quantum efficiency of the present LEDs; one is carrier/exciton localization[3,4] and the other is the quantum confinement Stark effect (QCSE)[5–7] which was caused by strong piezoelectric polarization in strained In$_x$Ga$_{1−x}$N/GaN quantum wells (QWs).[8,9] The former suppresses nonradiative processes to improve internal quantum efficiency, and the latter prevents the radiative recombination to degrade the efficiency. Furthermore, the QCSE becomes remarkable with increasing In composition in In$_x$Ga$_{1−x}$N/GaN QWs and, so, can be a major drawback for realizing LEDs operating at longer wavelengths. Therefore, it is crucially important for LEDs with higher performances to avoid the QCSE.

For this purpose, the use of nonpolar planes such as $M$-plane $(10\bar{1}0)$ or $A$-plane $(11\bar{2}0)$ has been proposed. In fact, a $(Al,Ga)N/GaN$ multiple quantum well (MQW) with a nonpolar $[10\bar{1}0]$ orientation was grown on $\gamma$-LiAlO$_2$ (100) substrate.[10] However, it is generally difficult to grow polar materials such as GaN on nonpolar substrates. A clue to another approach can be found in Refs. 11 and 12, in which the magnitude of piezoelectric fields (PFs) was calculated as a function of the tilt angle of the $c$-axis from the surface normal, and it was shown that PFs could be zero at 90° and 39°. The plane inclined 90° corresponds to nonpolar planes such as $M$- or $A$-plane, while 39° is very close to the angle formed by $(11\bar{2}4)$ and $(10\bar{1}2)$ planes. In these papers, QWs were grown on the inclined $(10\bar{1}1)$ facets but the QWs unexpectedly showed very weak luminescence due to the presence of a number of stacking faults.

From this background, in this study, we propose the regrowth technique, in which well-established and high quality $C$-oriented GaN on sapphire (0001) substrate is used as a seed. We demonstrate that the multiple quantum wells (MQWs) grown on $C$-oriented GaN patterned with a stripe along the $[1\bar{1}00]$ direction have the facets of (0001), $\{11\bar{2}2\}$, and $\{11\bar{2}0\}$, and that the $\{11\bar{2}2\}$ QWs involve weaker PFs and drastically improve the luminescence efficiency compared with conventional $C$-oriented In$_x$Ga$_{1−x}$N QWs.

The GaN template with a thickness of 4 $\mu$m was firstly grown on a (0001) sapphire substrate by metalorganic vapor-phase epitaxy under atmosphere pressure. A stripe pattern with a repetition of 20 $\mu$m was then formed along the $[1\bar{1}00]$ direction by a reactive ion etching (RIE) technique. The GaN template was deeply etched to the sapphire substrate. The stripe width was 4 $\mu$m and the sidewall is nonpolar $\{11\bar{2}0\}$ planes. A 1-$\mu$m-thick GaN layer was then grown on the patterned GaN to recover damage induced by the RIE process, and followed by the growth of three-period In$_x$Ga$_{1−x}$N/GaN MQWs. The well thickness and In composition of the QWs were analyzed by the cross-sectional scanning transmission electron microscopy (STEM) equipped with energy dispersive x-ray spectroscopy (EDS) (JEOL:JEM-2100F) and x-ray diffraction (XRD) measurements. The specimen for STEM was prepared by a conventional Ar ion milling technique, the thickness of which was about 100 nm or less. The acceleration voltage for STEM was 200 kV.

Microscopic photoluminescence (PL) was measured at room temperature (RT) using a confocal microscope, of which the spatial resolution was less than 500 nm. Both excitation and collection of PL were through a microscope objective lens, and therefore, the PL property of each growth facet could be assessed separately. The excitation pulses were from a frequency-doubled Ti:sapphire laser (Spectra Physics: TSUNAMI), of which the wavelength and excitation power density were 353 nm and 45.8 $\mu$J/cm$^2$, respectively. The PL was detected by a cooled head CCD camera.

In order to estimate the internal quantum efficiency and lifetimes of both radiative and nonradiative processes, temperature dependence of PL and time-resolved (TR) PL was

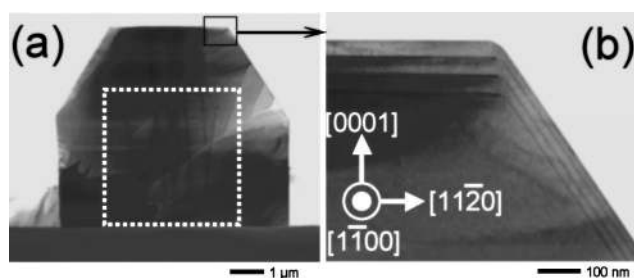[a]Electronic mail: k-nishi@fujita.kuee.kyoto-u.ac.jp

FIG. 1. Cross-sectional STEM images viewed from $[1\bar{1}00]$ direction. (a) Entire region and (b) magnified image of the (0001) and $\{11\bar{2}2\}$ facets. The white broken square indicates the shape of GaN before regrowth.
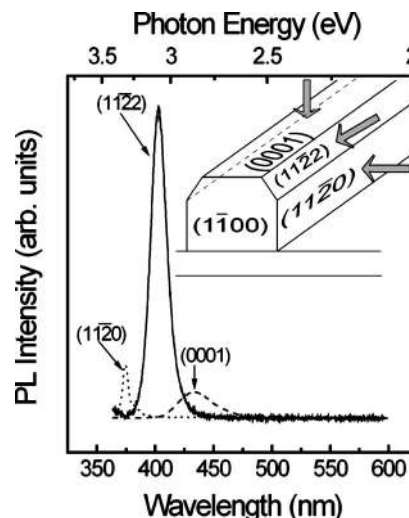


FIG. 2. Microscopic PL spectra from the $(11\bar{2}0)$, $(11\bar{2}2)$, and (0001) MQWs at RT. The inset figure shows the schematic sample structure, and arrows indicate the directions for excitation and collection.

investigated. The $In_xGa_{1-x}N$ well layers were selectively excited using excitation pulses with a wavelength of 380 nm from the frequency-doubled Ti:sapphire laser. The excitation energy density was 7.95 $\mu J/cm^2$. The sample was held in a cryostat, and luminescence was detected by a CCD camera or a streak camera.

Figure 1(a) shows a cross-sectional STEM image viewed from the $[1\bar{1}00]$ direction. It is clearly seen that the regrowth transforms the shape of the cross-section, and that two inclined facets as well as (0001) and $\{11\bar{2}0\}$ appear. These two facets form the same angle to (0001), and therefore, these are crystallographically equivalent. The angle was estimated to be 56°, indicating that the planes are $\{11\bar{2}2\}$. A very similar cross-sectional shape has already been reported for ELOG or facet-controlled ELO GaN.[13] These techniques use a $SiO_2$ mask on the top of a GaN template, while in this study, the sapphire substrate appearing between each GaN stripe works as a mask. According to Ref. 13, the shape strongly depends on the growth conditions such as growth temperature and pressure. The growth mechanism is still unclear, but phenomenologically it was pointed out that $\{11\bar{2}2\}$ facets tend to appear by decreasing the growth temperature and/or increasing the pressure. Since present sample was grown under atmospheric pressure, it is, thus, natural to have $\{11\bar{2}2\}$ facets.

The three-period $In_xGa_{1-x}N$ MQWs could be observed on all the facets. A magnified image of the (0001) and $\{11\bar{2}2\}$ facets is shown in Fig. 1(b), where the well and barrier layers make a striking contrast. That of the $\{11\bar{2}0\}$ facet is not shown, because the contrast can actually be seen, but it is not so clear due to a low In composition. The well and barrier thicknesses were estimated to be 6.1 and 38.6 nm for (0001), 2.8 and 17.2 nm for $\{11\bar{2}2\}$, and 2.2 and 17.4 nm for $\{11\bar{2}0\}$ QWs.

In order to estimate the In compositions in the well layers, XRD and EDS measurement were performed. It is difficult to evaluate true In compositions from EDS signals without a standard sample, and it is also difficult to measure XRD profiles of the $\{11\bar{2}2\}$ and $\{11\bar{2}0\}$ QWs under the present sample geometry. Therefore, both XRD and EDS were measured to complement each other. For the EDS measurement, line profiles of the In compositions across the MQWs were investigated. If the EDS signal was generated only within the incident electron beam, the line profile must be expressed by a delta function because the beam spot of 1 nm is narrower than the well widths. However, this does not fit the experimental results. Therefore, we considered that

the EDS signal was generated also around the electron beam, and assumed that the contribution could be expressed by a Gaussian distribution. A good fit with the line profiles could be attained by assuming a standard deviation of 1.75 nm. The In compositions shown subsequently were determined taking this distribution into account.

First, the XRD profile of the (0001) QW was taken in the vicinity of the (0002) diffraction. Satellite peaks were clearly seen, and the In compositions, well and barrier thicknesses were estimated to be 13.5%, 5.8 nm, and 32.1 nm, respectively, by a fit using the dynamical diffraction theory. The error seems very small because a 1% difference in the In composition caused a discernible difference between the simulated and the experimentally obtained XRD profiles. It is also worth nothing that the thickness determined by the XRD is more reliable than STEM. From the relative intensity of EDS signals for In, the In compositions of $\{11\bar{2}2\}$ and $\{11\bar{2}0\}$ QWs were calculated to be 7.5% and 2.4%, respectively. Using the obtained In compositions, the magnitude of electric fields due to piezoelectric and spontaneous polarizations were calculated to be 1.87 MV/cm for (0001), 0.53 MV/cm for $\{11\bar{2}2\}$, and 0 MV/cm for nonpolar $\{11\bar{2}0\}$ QWs. Taking these electric fields and quantum confinement effect into account, the transition energies of the (0001), $\{11\bar{2}2\}$, and $\{11\bar{2}0\}$ QWs at RT were evaluated to be 2.22, 3.15, and 3.39 eV, respectively. If the electric fields are totally screened, the transition energies could be 2.96 eV for (0001) and 3.23 eV for $\{11\bar{2}2\}$ MQWs.

The microscopic PL spectrum from each facet is shown in Fig. 2. The peaks from $(11\bar{2}0)$, $(11\bar{2}2)$, and (0001) QWs were observed at 3.31, 3.07, and 2.86 eV, respectively. Small deviations from the calculated transition energies may be due to the error in estimating In mole fractions, and/or to the partial screening of PFs induced by photogenerated carriers. The luminescence intensity is the strongest for the $(11\bar{2}2)$ QW and the weakest for the (0001) QWs. As was mentioned earlier, the (0001) QW has the strongest PFs and, furthermore, the widest well width, which leads to a lower transition probability. Therefore, it is reasonable that the PL inten-
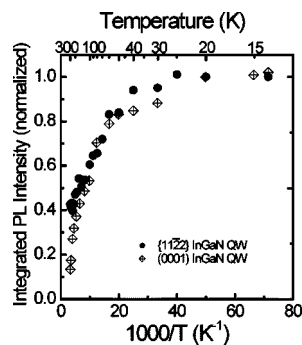
FIG. 3. Temperature dependence of integrated PL intensities of the $\{11\bar{2}2\}$ QW and the conventional $C$-oriented In$_x$Ga$_{1-x}$N QW. The intensities were normalized by those at 13 K.

sity from the (0001) QW is the weakest. For a comparison between the $(11\bar{2}2)$ and $(11\bar{2}0)$ QWs, the In compositions must be considered. The very low In composition in the $(11\bar{2}0)$ QWs of 2.4% weakens the confinement of carriers in the wells, and carriers can thermally escape from the wells to the barriers. Consequently, carriers do not recombine radiatively in the wells and the PL intensity becomes weak, compared with the $\{11\bar{2}2\}$ QWs. It should be noted that the PFs in the $\{11\bar{2}2\}$ QWs are predicted rather weak, which also contributes to the enhancement of the PL intensity.

In order to assess the internal quantum efficiency in the $\{11\bar{2}2\}$ QW, the temperature dependence of PL was measured. The variation of the integrated PL intensity is shown in Fig. 3, in which result for a conventional $C$-oriented In$_x$Ga$_{1-x}$N QWs emitting at a similar wavelength of about 400 nm is also shown for a comparison. Neglecting nonradiative recombination processes at low temperature, the internal quantum efficiency at low temperatures can be regarded as 100% and that at elevated temperatures can be evaluated from the PL intensity ratio. The internal quantum efficiency of $\{11\bar{2}2\}$ QW at RT was thus estimated about 40%. This value is about three times as high as that of the conventional $C$-oriented QW, as shown in Fig. 3. This is probably due to the internal PFs in the $\{11\bar{2}2\}$ QWs weaker than that in the $C$-oriented In$_x$Ga$_{1-x}$N QWs, which makes electron–hole recombination probability higher.

It is generally true that when the well width is thin, the internal electric field in the well does not affect the PL peak positions. As a matter of fact, our $\{11\bar{2}2\}$ QW having the
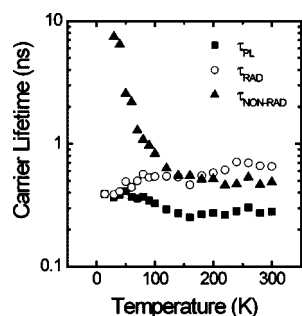
well as thin as 2.8 nm and the $C$-oriented QW showed almost identical blue shift of the PL peaks when the excitation power was changed from 0.27 to 19.0 $\mu$J/cm$^2$. (The blueshift can be attributed to the band filling effect of localized states.) On the other hand, a theoretical study showed that exciton spontaneous emission lifetime is strongly affected by the presence of electric fields even in a well as thin as 1 nm.[14] This theoretical study tells us that, if the electric field in the $\{11\bar{2}2\}$ QW is surely weakened, a fast radiative recombination lifetime should be observed. To confirm this assertion, the temperature dependence of TRPL was measured for the $\{11\bar{2}2\}$ QW, and with Fig. 3, the temperature dependences of radiative ($\tau_{RAD}$) and nonradiative ($\tau_{NON-RAD}$) lifetimes were extracted. Figure 4 shows the summary. The radiative lifetime of the $\{11\bar{2}2\}$ QW is slightly changed from 0.38 to 0.65 ns upon increasing the measurement temperature, while another experiment showed that of the $C$-oriented In$_x$Ga$_{1-x}$N QWs with a 3 nm well emitting at a similar wavelength was 1.43 ns at low temperatures. The much faster lifetime for the $\{11\bar{2}2\}$ QW provides strong evidence for the reduction of the electric fields in the $\{11\bar{2}2\}$ QW. The internal quantum efficiency is expressed as $1/(1+\tau_{RAD}/\tau_{NON-RAD})$, and thus, that of the $\{1122\}$ was enhanced compared with $C$-oriented InGaN QWs.

FIG. 4. Temperature dependence of PL decay times ($\tau_{PL}$), radiative ($\tau_{RAD}$), and nonradiative ($\tau_{NON-RAD}$) lifetimes.

[1]S. Nakamura, M. Senoh, N. Iwasa, and S. Nagahama, Jpn. J. Appl. Phys., Part 2 **34**, L797 (1995).

[2]S. Nakamura, M. Senoh, N. Iwasa, and S. Nagahama, T. Yamada, and T. Mukai, Jpn. J. Appl. Phys., Part 2 **34**, L1132 (1995).

[3]S. Chichibu, T. Azuhara, T. Sota, and S. Nakamura, Appl. Phys. Lett. **69**, 4188 (1996).

[4]Y. Narukawa, Y. Kawakami, M. Funato, S. Fujita, S. Fujita, and S. Nakamura, Appl. Phys. Lett. **70**, 981 (1997).

[5]P. Perlin, C. Kisielowski, V. Iota, B. A. Weinstein, L. Mattos, N. A. Shapiro, J. Kruger, E. R. Weber, and J. Yang, Appl. Phys. Lett. **73**, 2778 (1998).

[6]T. Takeuchi, S. Sota, M. Katsuragawa, M. Komori, H. Takeuchi, H. Amano, and I. Akasaki, Jpn. J. Appl. Phys., Part 2 **36**, L382 (1997).

[7]T. Takeuchi, C. Wetzel, S. Yamaguchi, H. Sakai, H. Amano, I. Akasaki, Y. Kaneko, S. Nakagawa, Y. Yamaoka, and N. Yamada, Appl. Phys. Lett. **73**, 1691 (1998).

[8]C. Wetzel, T. Takeuchi, S. Yamaguchi, H. Katoh, H. Amamo, and I. Akasaki, Appl. Phys. Lett. **73**, 1994 (1998).

[9]T. Takeuchi, C. Wetzel, S. Yamaguchi, H. Sakai, H. Amano, I. Akasaki, Y. Kaneko, Y. Yamaoka, S. Nakagawa, and N. Yamada, Appl. Phys. Lett. **73**, 1691 (1998).

[10]P. Waltereit, O. Brandt, A. Trampert, H. T. Grahn, J. Menniger, M. Ramsteiner, M. Reiche, and K. H. Ploog, Nature (London) **406**, 865 (2000).

[11]T. Takeuchi, S. Lester, D. Basile, G. Girolami, R. Twist, F. Mertz, M. Wong, R. Schneider, A. Amano, and I. Akasaki, Proc. Int. Workshop on Nitride Semiconductors, IPAP Conf. I, 2000, p. 137.

[12]T. Takeuchi, A. Amano, and I. Akasaki, Jpn. J. Appl. Phys., Part 1 **39**, 413 (2000).

[13]K. Hiramatsu, K. Nishiyama, M. Onishi, H. Mizutani, M. Narukawa, A. Motogaito, H. Miyake, Y. Iyechika, and T. Maeda, J. Cryst. Growth **221**, 316 (2000).

[14]M. Funato, Y. Kawaguchi, and Sg. Fujita, Mater. Res. Soc. Symp. Proc. 789, Y10.12 (2004).